

# Woven Constructions for Multi-Level Information Protection<sup>1</sup>

R.Johannesson\*, V.Pavlushkov\*, V.V.Zyablov\*\*

\*Department of Information Technology Lund University

P.O. Box 118, SE-22100 Lund, Sweden, e-mail: {rolf; victor}@it.lth.se

\*\*Institute for Information Transmission Problems, Russian Academy of Sciences

B. Karetnyi per. 19, GSP-4, 101447 Moscow, Russia, e-mail: zyablov@iitp.ru

Received April, 25, 2005

**Abstract**—Many communication systems require transmission of certain parts of the information symbols with lower decoding bit error probabilities than others. Using the system requirements for an actual project as an example, two encoding schemes, namely, a woven convolutional scheme and a woven turbo scheme, were simulated with iterative decoding. The simulation results for both schemes confirm the presence of unequal error protection and demonstrate their good error-correcting performance, despite the fact that no optimization was done.

## 1. INTRODUCTION AND PROBLEM DESCRIPTION

The Russian Foundation for Basic Research has announced the project 05-01-00778 with the purpose to build a radio-telescope by using a satellite revolving around the Earth. While traveling along its orbit, the satellite sends observed data to the ground control stations. According to the system specifications, the down-link communication from the satellite to a ground station consists essentially of two parts of information: 95% is the telescope data itself and 5% is control data. The communication system should provide a probability of decoding error for the control data as low as  $P_{b,1} \leq 10^{-5}$ , while for the telescope data it is enough to have  $P_{b,2} \leq 10^{-2}$ . The length of a packet should be between 100,000 and 150,000 code symbols. This implies that if a convolutional scheme is in use, then the code sequences have to be terminated after such a length.

In this paper we investigate two encoding schemes, *viz.*, a woven convolutional scheme and a woven turbo scheme, that provide two-level unequal error protection for the information symbols such that the system requirements are satisfied.

As a reference we use the communication system with uncoded transmission. To transmit an information bit with the required reliability over the down-link channel one has to supply the following average energy per information bit

$$E_{b,\text{uncoded}} = 0.05E_{b,1} + 0.95E_{b,2} \quad (1)$$

where energy  $E_{b,1}$  corresponds to  $P_{b,1} = 10^{-5}$  and  $E_{b,2}$  corresponds to  $P_{b,2} = 10^{-2}$ . For space communication, the channel can be very well modeled as a channel with additive white Gaussian noise (AWGN). Then, for a system with binary phase-shift keying (BPSK) modulation we have  $E_{b,1}/N_0 = 9.59$  dB and  $E_{b,2}/N_0 = 4.32$  dB, which yield  $E_{b,\text{uncoded}}/N_0 = 4.81$  dB.

<sup>1</sup> This research was supported in part by the Royal Swedish Academy of Sciences in cooperation with the Russian Academy of Sciences, by the Swedish Research Council under Grant 2003-3262, by the Russian Foundation for Basic Research under Project 05-01-00778, and by the Graduate School in Personal Computing and Communication PCC++.

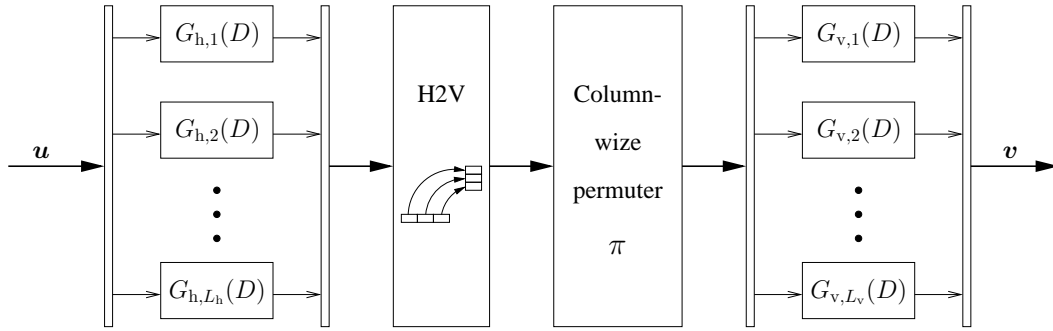


Figure 1. A woven convolutional encoder.

2. ENCODING SCHEMES

It was shown in [1,2] that encoding schemes with warps are suitable for achieving unequal error protection for both information and code symbols. Thus, we consider two schemes with a warp, viz., a woven convolutional encoder and a woven turbo encoder, and compare their error-correcting performances.

2.1. Woven Convolutional Encoders

Woven convolutional codes were presented and studied in [3,4]. In this paper, we use a modification of a woven convolutional encoder which was considered in [2]. The encoder construction is shown in Figure 1. For simplicity, we assume that the constituent encoders which provide the better error-correcting capability are located on the first  $L_{h,b}$  positions in the outer warp. Furthermore, let the inner warp consist of  $L_v$  identical constituent encoders.

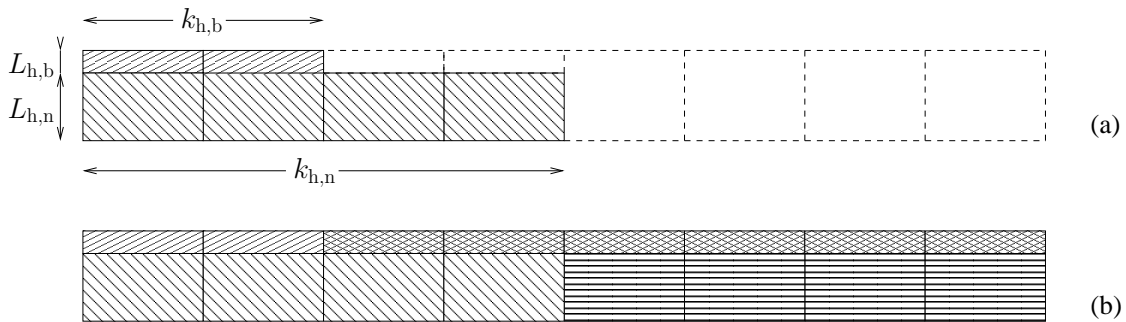
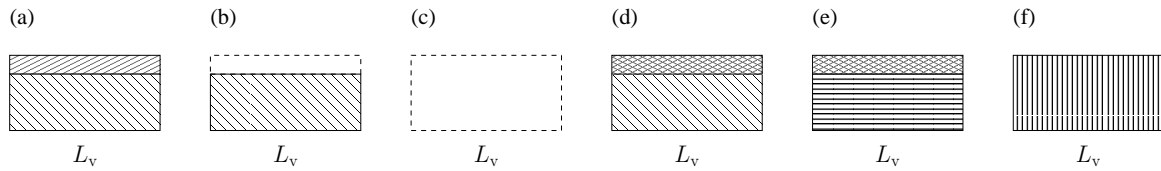
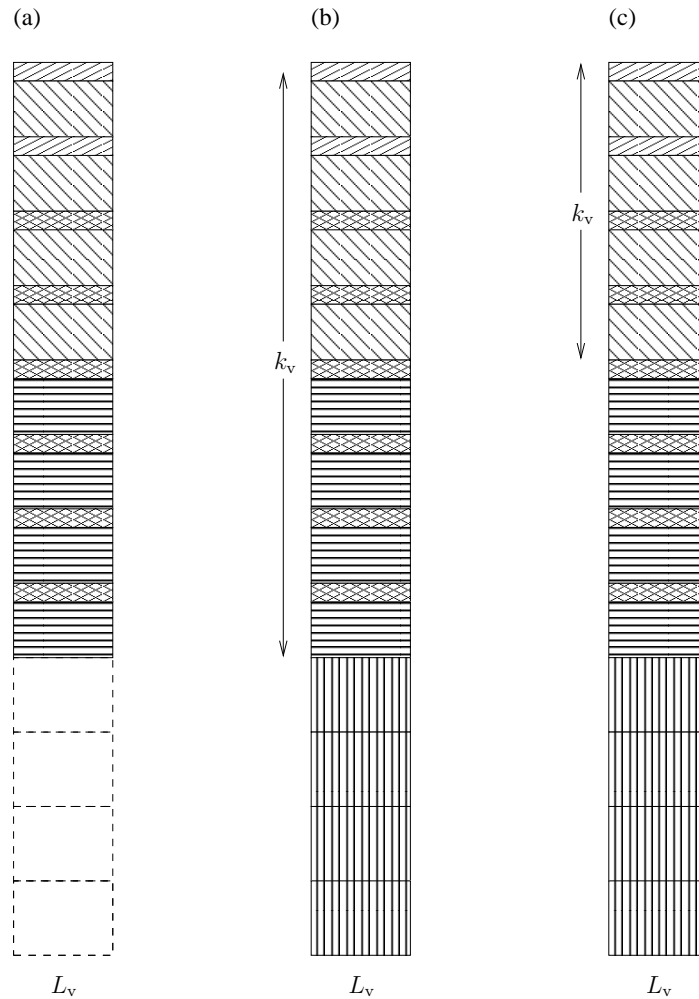


Figure 2. Horizontal systematic encoding: (a) the structure of an information block and (b) the structure of the corresponding encoded block with horizontal parity symbols filling the empty room.

During the “horizontal” encoding, the first stage of woven encoding, the information is distributed over the constituent encoders in the outer warp, feeding the first  $L_{h,b}$  constituent encoders with information to be better protected against channel errors, while the other  $L_{h,n}$  constituent encoders are responsible for the normally protected information symbols. According to the system requirements, we terminate the information sequence, although, in general, it is not necessary for a woven convolutional encoder. Thus, in this case, the woven convolutional encoder can be considered as a rate  $R = K/N$  block encoder. The information symbols are written in a block structure as shown in Figure 2(a) with the symbols to be better protected occupying the first  $L_{h,b}$  rows. Each row is independently encoded by an individual constituent systematic outer encoder and the obtained parity symbols fill the empty room as illustrated in Figure 2(b). The information symbols in



**Figure 3.** Elementary sub-blocks: (a) an information sub-block with  $L_{h,b}$  rows to be better protected and  $L_{h,n}$  rows to be normally protected, (b) an information sub-block with only  $L_{h,n}$  rows, (c) an empty sub-block reserved for parity symbols, (d) a sub-block with horizontal parity symbols for the better protected first  $L_{h,b}$  rows and information symbols in the remaining  $L_{h,n}$  rows, (e) a sub-block with horizontal parity symbols for both better and normally protected rows, and (f) a sub-block with vertical parity symbols.



**Figure 4.** Vertical systematic encoding in woven schemes: (a) the structure of a block after horizontal encoding and H2V rearrangement, (b) and (c) are the structure of the corresponding block after vertical, systematic encoding in the woven convolutional and the woven turbo encoder, respectively.

the first  $L_{h,b}$  rows are encoded by constituent encoders with lower rate which correspond to more parity symbols (per row). That is why these rows have information segments of length  $k_{h,b}$ , which is shorter than the length  $k_{h,n}$  in the remaining  $L_{h,n}$  rows.

After this encoding, the resulting block is subdivided into sub-blocks of length  $L_v$  symbols. For simplicity, assume that both  $k_{h,b}$  and  $k_{h,n}$  are multiples of  $L_v$ . The elementary sub-blocks appearing in the schemes are explained in Figure 3. The horizontal-to-vertical (H2V) transformation

rearranges these sub-blocks vertically as shown in Figure 4(a). If the lengths  $k_{h,b}$  and  $k_{h,n}$  are matched to the rates of the corresponding constituent outer encoders,  $R_{h,b}$  and  $R_{h,n}$ , respectively, that is, if

$$\frac{k_{h,b}}{R_{h,b}} = \frac{k_{h,n}}{R_{h,n}} \quad (2)$$

then the height of the pile of sub-blocks is

$$k_v = \frac{k_{h,n}(L_{h,b} + L_{h,n})}{L_v R_{h,n}}. \quad (3)$$

In all the simulated schemes these values are matched.

After the horizontal-to-vertical transformation we perform a column-wise permutation  $\pi$  and the resulting block is fed to the inner warp, for the so-called “vertical” encoding. Each column is independently encoded by an individual constituent systematic inner encoder with parity symbols filling the reserved room at the pile’s bottom. This encoding stage is schematically shown in Figure 4(b). Note that in this figure we have skipped the preceding column-wise permutation  $\pi$  in order to make the illustration of the structure more clear.

Neglecting the termination length, the overall rate of the woven convolutional encoder is

$$R = \frac{K}{N} = \frac{k_{h,b}L_{h,b} + k_{h,n}L_{h,n}}{\left(\frac{k_{h,b}L_{h,b}}{R_{h,b}} + \frac{k_{h,n}L_{h,n}}{R_{h,n}}\right) \frac{1}{R_v}} \quad (4)$$

where  $R_{h,b}$  and  $R_{h,n}$  are the rates of the constituent outer (horizontal) encoders for better and normally protected information symbols, respectively, and  $R_v$  is the rate of the constituent inner (vertical) encoders.

## 2.2. Woven Turbo Encoders

The woven turbo encoder was first introduced by Freudenberger *et al.* in [5]. This scheme combines the ideas of woven convolutional encoders and turbo encoders [6], and is basically a turbo encoder with warps of constituent encoders instead of single encoders. Here, we consider a slightly modified woven turbo encoder.

An information sequence  $\mathbf{u}$  is first organized in a block structure as in Figure 2(a) and encoded row-wise in the same way as for the woven convolutional encoders. Due to the termination, the whole scheme behaves as a rate  $R = K/N$  block encoder. The systematic horizontal encoding in the woven turbo encoder is schematically illustrated in Figure 2. After the horizontal encoding, the resulting block is subdivided into sub-blocks of width  $L_v$  symbols, that, in turn, are rearranged by the H2V transformation into a vertical pile as shown in Figure 4(a). In contrast to what we had for the woven convolutional encoder, the column-wise permutation  $\pi$  and the vertical encoding are performed only over the upper located “systematic” symbols until the end of the information part. If  $k_{h,n}$  is a multiple of  $L_v$  and (2) is fulfilled, then for this scheme the

$$k_v = \frac{k_{h,n}}{L_v} (L_{h,b} + L_{h,n}) \quad (5)$$

topmost symbols in every column are involved.

After the permutation, these “systematic” symbols are independently encoded column-wise by constituent systematic encoders with “vertical” parity symbols added under the “horizontal” parity symbols as shown in Figure 4(c). Again, the effect of the permutation is skipped in this illustration. Note that only a part of the parity symbols for the better protected information symbols is further

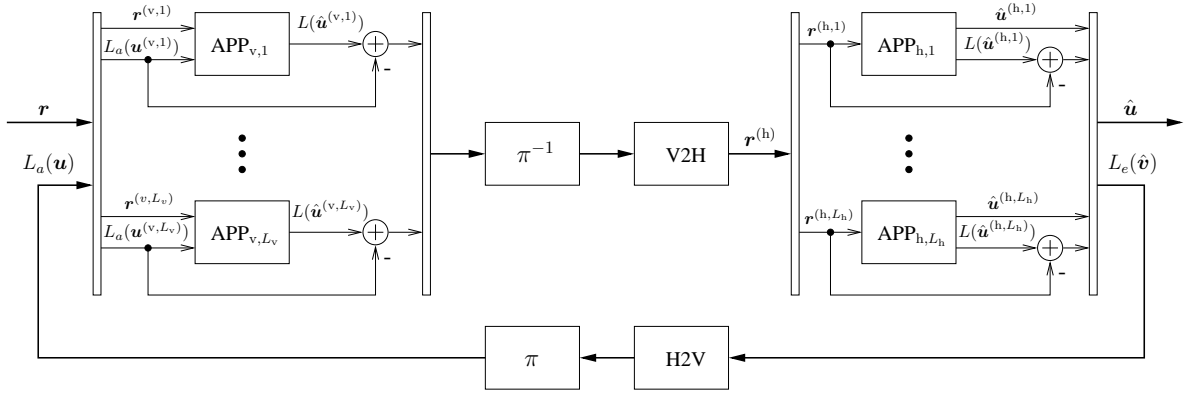


Figure 5. A decoder structure for a woven convolutional code.

encoded by the vertical encoders, which makes a representation of this encoder similar to Figure 1 very complicated. The systematic, horizontal and vertical parts of a codeword will be denoted as  $\mathbf{v}_s$ ,  $\mathbf{v}_-$ , and  $\mathbf{v}_{||}$ , respectively. Neglecting the termination lengths, the overall rate for this woven turbo encoder is given by

$$R = \frac{K}{N} = \frac{k_{h,b}L_{h,b} + k_{h,n}L_{h,n}}{\frac{k_{h,b}L_{h,b}}{R_{h,b}} + \frac{k_{h,n}L_{h,n}}{R_{h,n}} + k_vL_v \left( \frac{1}{R_v} - 1 \right)}. \tag{6}$$

### 3. DECODING

Since a warp in a woven encoder typically consists of a couple of dozens constituent encoders, the maximum-likelihood (ML) decoder for such a scheme is simply unfeasible. Thus, we use an iterative decoding procedure in our simulations.

#### 3.1. Decoding of Woven Convolutional Codes

The structure of a decoder for a woven convolutional code is shown in Figure 5. A received sequence  $\mathbf{r}$  is first distributed over the constituent “vertical” *a posteriori* probability (APP) decoders, corresponding to the encoding matrices  $G_{v,i}(D)$ ,  $i = 1, 2, \dots, L_v$ , in the woven convolutional encoder. Every constituent decoder independently decodes its portion of the received sequence  $\mathbf{r}^{(v,i)}$ ,  $i = 1, 2, \dots, L_v$ . After subtracting the *a priori* values  $L_a(\mathbf{u}^{(v,i)})$ , the resulting sequences are written column-wise organizing the block structure shown in Figure 4(a). Each column is then independently permuted by the inverse permuter  $\pi^{-1}$ . Then follows the vertical-to-horizontal (V2H) transformation, that is, the inverse of the H2V transformation, which subdivides the pile into elementary sub-blocks of hight  $L_h = L_{h,b} + L_{h,n}$  and puts them in a row. This results in a block  $\mathbf{r}^{(h)}$  structured as depicted in Figure 2(b). Feeding it row-wise to the constituent individual “horizontal” decoders and performing the APP decoding of each portion  $\mathbf{r}^{(h,i)}$ ,  $i = 1, 2, \dots, L_h$ , we obtain the decision on the transmitted information sequence  $\hat{\mathbf{u}}$  for a current iteration as well as the *a posteriori* values  $L_e(\hat{\mathbf{v}})$  that, after appropriate transformation by H2V and permutation  $\pi$ , will be used as *a priori* values  $L_a(\mathbf{u}^{(v,i)})$  in next iteration. After a predetermined number of iterations we stop decoding.

#### 3.2. Decoding of Woven Turbo Codes

The structure of a decoder for a woven turbo code is very similar to that for a woven convolutional code as can be seen from Figure 6. The only difference is caused by the fact that a received word  $\mathbf{r}$

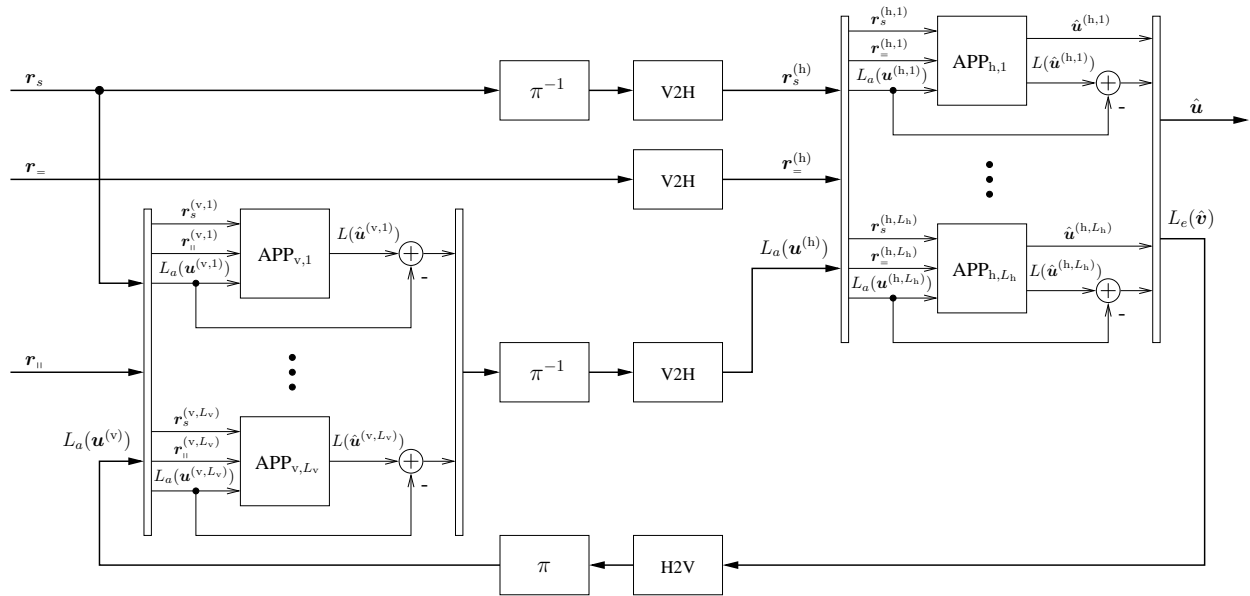


Figure 6. A decoder structure for a woven turbo code.

consists now of three parts—a “systematic” part  $r_s$ , a “horizontal” parity part  $r_v$ , and a “vertical” parity part  $r_h$  that are structured as shown in Figure 4(c). The systematic part  $r_s$  is provided to both warps of the constituent APP decoders, while  $r_v$  and  $r_h$  appear only at the inputs of the horizontal warp and the vertical warp, respectively.

First, being combined,  $r_s$  and  $r_h$  are decoded column-wise by the “vertical” constituent APP decoders. The resulting *a posteriori* values, after the V2H transformation, are used as *a priori* values  $L_a(\mathbf{u}^{(h)})$  for the horizontal decoding stage. Then,  $r_s$  is permuted by  $\pi^{-1}$  and together with  $r_v$  is rearranged by the V2H transformation to get the structure as shown in Figure 2(b). Feeding the symbols row-wise and independently performing decoding by the “horizontal” constituent APP decoders we obtain the decision on the transmitted information  $\hat{\mathbf{u}}$  for current iteration and the *a posteriori* values, that, after the H2V transformation and the permutation  $\pi$ , will be used by the “vertical” decoders as the *a priori* information during next iteration. After a predetermined number of iterations the decoding is over.

#### 4. SIMULATION RESULTS

In this section we consider the results of the simulations for both the woven convolutional encoder and the woven turbo encoder that were performed in order to choose the one that fits better to the system requirements and to illustrate the main features of the preferred scheme.

During the simulations the all-zero codeword was transmitted over an AWGN channel model. All the schemes are simulated until 50 packets are decoded erroneously at the receiver. Unless otherwise stated, a decoding procedure with 10 iterations was performed.

##### 4.1. Comparison of the Two Woven Schemes

First we compare the bit error probabilities for both the woven convolutional (WCC) scheme and for the woven turbo (WTC) scheme. The parameters for the simulated schemes are presented in Table 1. The two schemes have similar parameters and the only difference between them is the vertical encoding matrix, which has lower rate in the woven turbo encoder. This difference

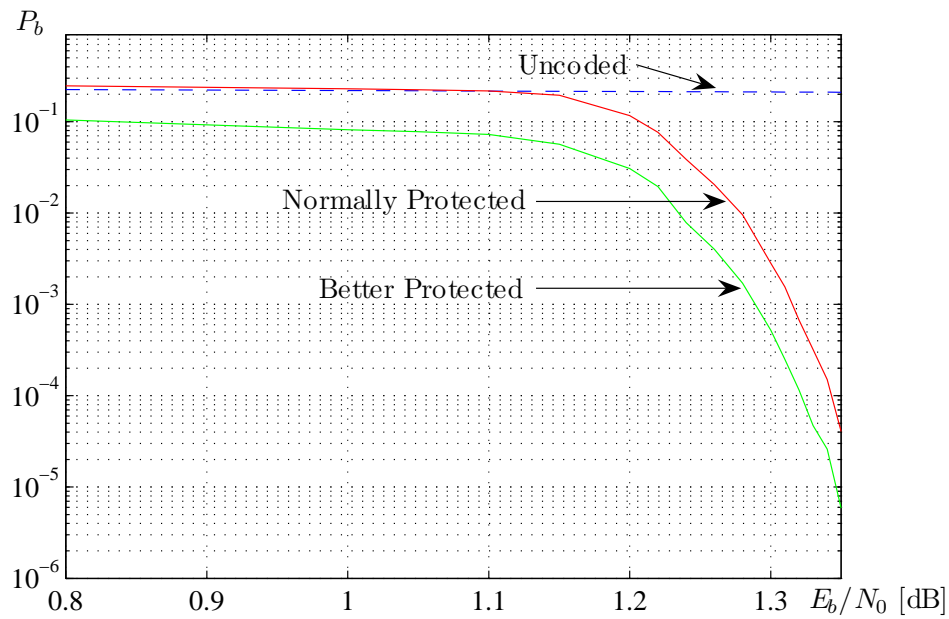


**Figure 7.** Bit error probabilities for the normally protected information symbols (red) and for the better protected information symbols (green) in the woven convolutional scheme of rate  $R \approx 0.24$ .

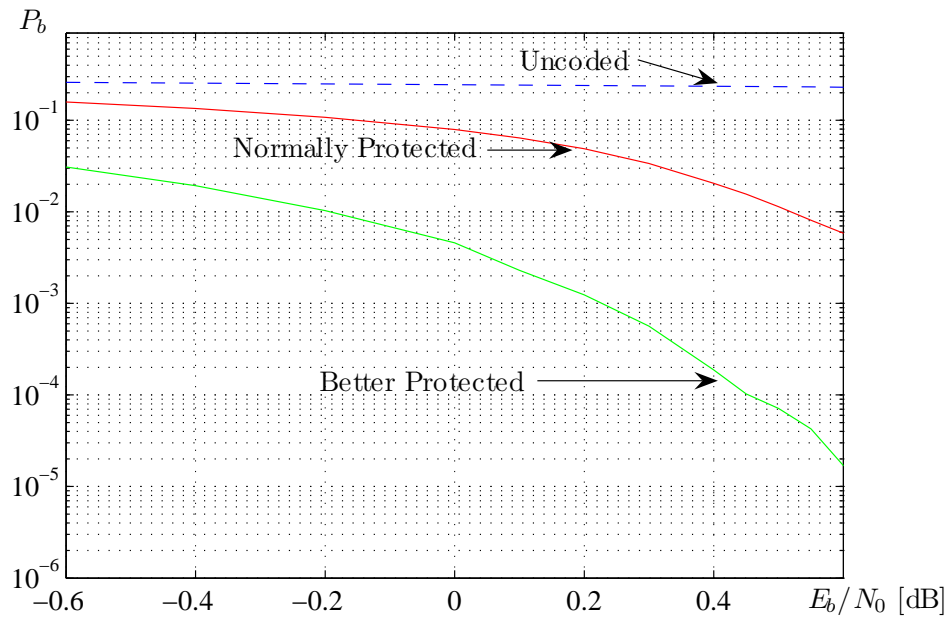


**Figure 8.** Bit error probabilities for the normally protected information symbols (red) and for the better protected information symbols (green) in the woven turbo scheme of rate  $R \approx 0.24$ .

is compensated by the fact that in woven turbo scheme, during the vertical encoding we do not encode the parity symbols from the horizontal encoding.

The resulting curves for bit error probabilities of normally protected information symbols and better protected information symbols are shown in Figures 7 and 8. Both woven schemes provide two-level unequal error protection for information symbols. However, they perform slightly different. The woven convolutional scheme seems to have a larger free distance as its bit error rate curves are much steeper as the channel becomes better than those of the woven turbo scheme. On the other hand, in the region of moderate signal-to-noise ratios, the woven turbo scheme works better.

	WCC	WTC
$k_{h,b}$	900	900
$k_{h,n}$	1800	1800
$k_v$	3600	1800
$L_{h,b}$	2	2
$L_{h,n}$	18	18
$L_v$	20	20
$G_{h,b}(D)$	$\left(1 \frac{D+D^2}{1+D+D^2} \frac{1+D^2}{1+D+D^2} \frac{1+D}{1+D+D^2}\right)$	
$G_{h,n}(D)$	$\left(1 \frac{1+D^2}{1+D+D^2}\right)$	
$G_v(D)$	$\left(1 \frac{1+D^2}{1+D+D^2}\right)$	$\left(1 \frac{D+D^2}{1+D+D^2} \frac{1+D^2}{1+D+D^2}\right)$
$K$	34200	34200
$N$	144000	144000
$R$	$\approx 0.24$	$\approx 0.24$

**Table 1.** Simulated system parameters for the woven convolutional and the woven turbo schemes of rate  $R \approx 0.24$ .

In our simulations, the woven turbo scheme achieves the desired levels  $P_b = 10^{-2}$  for the normally protected symbols and  $P_b = 10^{-5}$  for the better protected symbols at  $E_b/N_0 = 0.64$  dB, while the woven convolutional scheme satisfies the requirements only at  $E_b/N_0 = 1.35$  dB. Hence, the woven turbo scheme outperforms its competitor by 0.71 dB.

Since the system with uncoded transmission requires the signal-to-noise ratio  $E_{b,\text{uncoded}}/N_0 = 4.81$  dB, our woven schemes provide the coding gains of 4.17 dB and 3.46 dB, respectively. It is worth mentioning that the Shannon limit [7, 8] for rate  $R = 0.24$  is  $E_b/N_0 = -0.827$  dB. Thus, for the woven convolutional scheme we are less than 2.2 dB away from the Shannon limit; and that for the woven turbo scheme it is less than 1.5 dB away.

Since for the given system requirements this woven turbo scheme is more advantageous we consider only woven turbo schemes in sequel.

#### 4.2. Woven Turbo Encoders of Different Rates

Next we increase the rate of the scheme by changing the vertical encoder to one of rate  $R = 1/2$  and compare its performance with our previous woven turbo scheme. The simulated parameters for these two woven turbo schemes are compared in Table 2 and the bit error rate curves are plotted in Figure 9.

The simulations show that the scheme of rate  $R \approx 0.32$  satisfies the system requirements at  $E_b/N_0 = 0.55$  dB, while the one of rate  $R \approx 0.24$  does it a tenth of a dB later, *viz.*, at  $E_b/N_0 = 0.65$  dB. Thus, the former scheme provides simultaneously larger transmission rate and (slightly) better bit error rate performance. Increasing the overall rate further requires encoders with larger number of inputs, which increases the complexity of constituent decoders.

Comparing this scheme with the system with uncoded transmission, we conclude that the coding gain for the woven turbo scheme of rate  $R \approx 0.32$  is at least 4.25 dB. The Shannon limit for rate  $R = 0.32$  is  $E_b/N_0 = -0.544$  dB. Then, at  $P_b = 10^{-5}$ , this scheme is less than 1.1 dB away from the Shannon limit. Thus, with the woven turbo scheme of rate  $R \approx 0.32$  we are about 0.4 dB closer to the Shannon limit than with the one of rate  $R \approx 0.24$ .

We use this woven turbo scheme of rate  $R \approx 0.32$  as the basis for our investigations.

$k_{h,b}$	900	900
$k_{h,n}$	1800	1800
$k_v$	1800	1800
$L_{h,b}$	2	2
$L_{h,n}$	18	18
$L_v$	20	20
$G_{h,b}(D)$	$\left(1 \frac{D+D^2}{1+D+D^2} \frac{1+D^2}{1+D+D^2} \frac{1+D}{1+D+D^2}\right)$	
$G_{h,n}(D)$	$\left(1 \frac{1+D^2}{1+D+D^2}\right)$	
$G_v(D)$	$\left(1 \frac{D+D^2}{1+D+D^2} \frac{1+D^2}{1+D+D^2}\right)$	$\left(1 \frac{1+D^2}{1+D+D^2}\right)$
$K$	34200	34200
$N$	144000	108000
$R$	$\approx 0.24$	$\approx 0.32$

**Table 2.** Simulated system parameters for two woven turbo schemes of rate  $R \approx 0.24$  and rate  $R \approx 0.32$ , respectively.

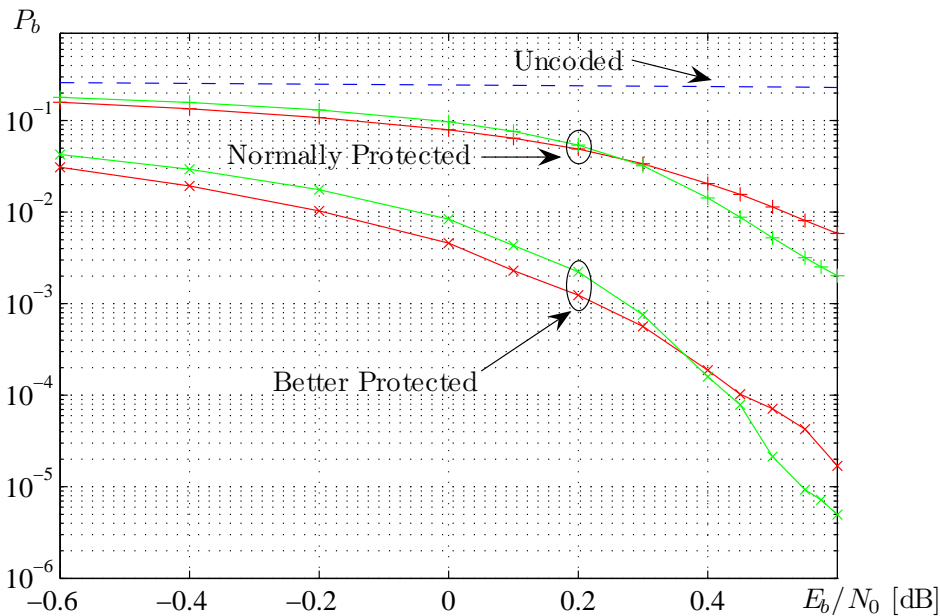


**Figure 9.** Bit error probabilities for the woven turbo schemes of rate  $R \approx 0.24$  (red) and rate  $R \approx 0.32$  (green), respectively.

#### 4.3. Equal Protection

When separating a portion of information symbols and providing better protection for them, there is always a danger to weaken the performance of the system for the normally protected symbols. That is why we also compare our woven turbo scheme with a scheme consisting of identical constituent encoders in the warp, which provides equal error protection (EEP) for the information symbols. The parameters for both schemes are collected in Table 3 and the resulting bit error probabilities are plotted in Figure 10.

The curves show that when introducing unequal error protection we indeed decrease the system performance for the normally protected information symbols by 0.1 dB in the depicted region. However, due to the scheme's performance for the better protected information symbols, we have

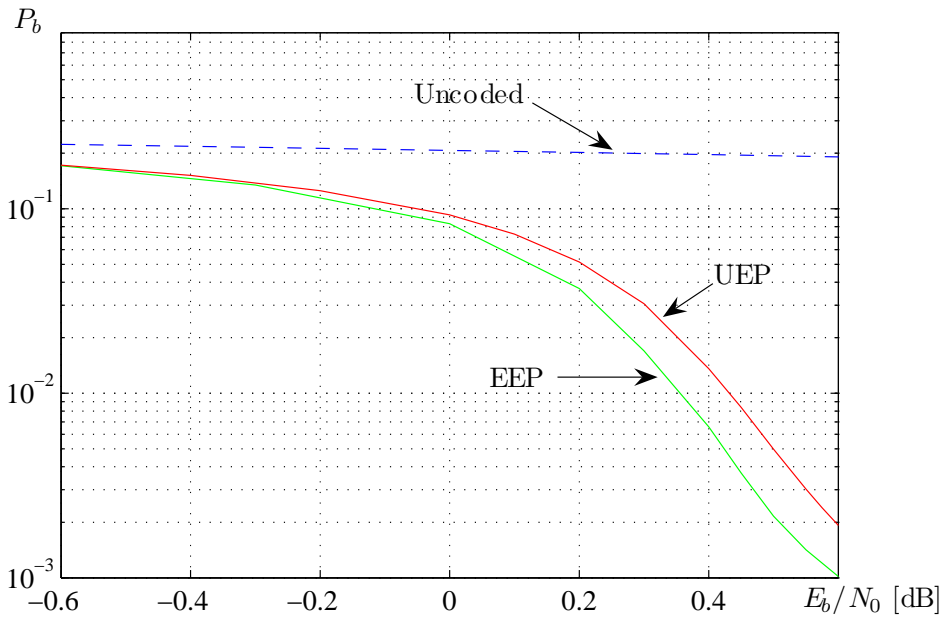


**Figure 10.** Bit error probabilities for the woven turbo scheme with (red) and without (green) unequal error protection.

	UEP	EEP
$k_{h,b}$	900	900
$k_{h,n}$	1800	1800
$k_v$	1800	1800
$L_{h,b}$	2	0
$L_{h,n}$	18	20
$L_v$	20	20
$G_{h,b}(D)$	$\left(1 \frac{D+D^2}{1+D+D^2} \frac{1+D^2}{1+D+D^2} \frac{1+D}{1+D+D^2}\right)$	
$G_{h,n}(D)$	$\left(1 \frac{1+D^2}{1+D+D^2}\right)$	
$G_v(D)$	$\left(1 \frac{1+D^2}{1+D+D^2}\right)$	
$K$	34200	36000
$N$	108000	108000
$R$	$\approx 0.32$	$\approx 0.33$

**Table 3.** Simulated system parameters for the woven turbo scheme with and without unequal error protection, respectively.

to provide  $E_b/N_0 = 0.55$  dB, where both schemes easily achieve the required  $P_b = 10^{-2}$  for the normally protected symbols. Thus, the normally protected information symbols can be considered essentially undisturbed by the better protected symbols.

#### 4.4. Different Warp Sizes

How does varying the size of the warps affect the system performance? As specified in Table 4, three woven turbo schemes with warp sizes  $L_h = L_v = 10$ ,  $L_h = L_v = 20$ , and  $L_h = L_v = 30$  were simulated. The corresponding bit error probabilities are shown in Figure 11.

$k_{h,b}$	1800	900	600
$k_{h,n}$	3600	1800	1200
$k_v$	3600	1800	1200
$L_{h,b}$	1	2	3
$L_{h,n}$	9	18	27
$L_v$	10	20	30
$G_{h,b}(D)$	$\left(1 \frac{D+D^2}{1+D+D^2} \frac{1+D^2}{1+D+D^2} \frac{1+D}{1+D+D^2}\right)$		
$G_{h,n}(D)$	$\left(1 \frac{1+D^2}{1+D+D^2}\right)$		
$G_v(D)$	$\left(1 \frac{1+D^2}{1+D+D^2}\right)$		
$K$	34200	34200	34200
$N$	108000	108000	108000
$R$	$\approx 0.32$	$\approx 0.32$	$\approx 0.32$

**Table 4.** Simulated system parameters for the woven turbo schemes with different warp sizes.

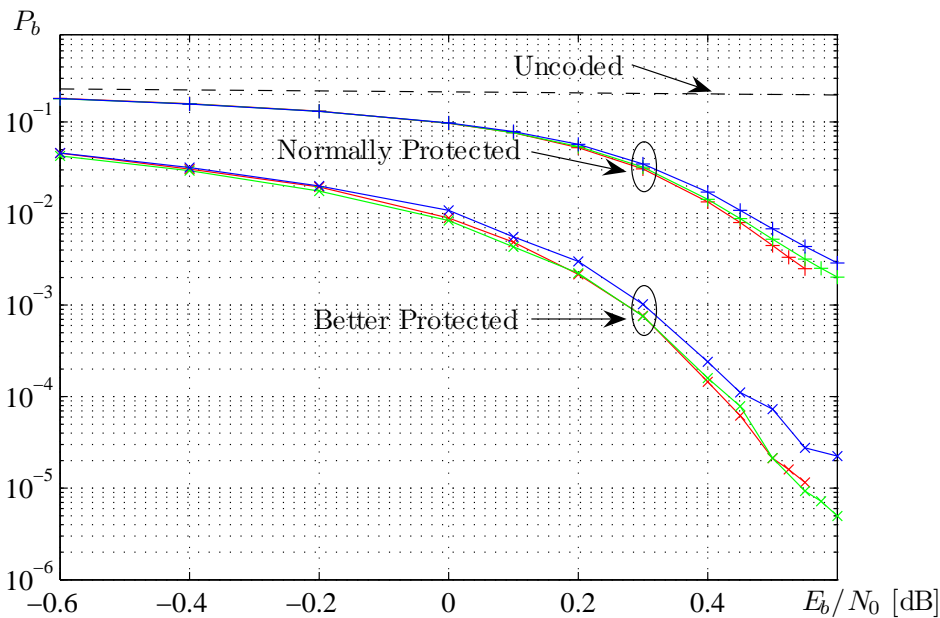


**Figure 11.** Bit error probabilities for the simulated woven turbo schemes with segment lengths  $L_h = L_v = 10$  (red),  $L_h = L_v = 20$  (green), and  $L_h = L_v = 30$  (blue), respectively.

The curves for warp sizes of 10 and 20 are almost identical, while the scheme with 30 constituent encoders in every warp performs a little bit worse. A possible explanation for this is that with larger warp size the permuter size becomes shorter and from some point it is not enough for good permutation. Based on this reasoning, it is rather tempting to decrease the size of warps. However, for our scheme it is impossible as a smaller number of constituent encoders does not allow us to subdivide the information symbols in the desired proportion.

#### 4.5. Effects of Permutations

It is not a good idea to exclude permutations in a turbo scheme and, in fact, the classical turbo encoders do not work without permutations. Computing the woven turbo scheme with and without permutations between the warps yields the results shown in Figure 12.

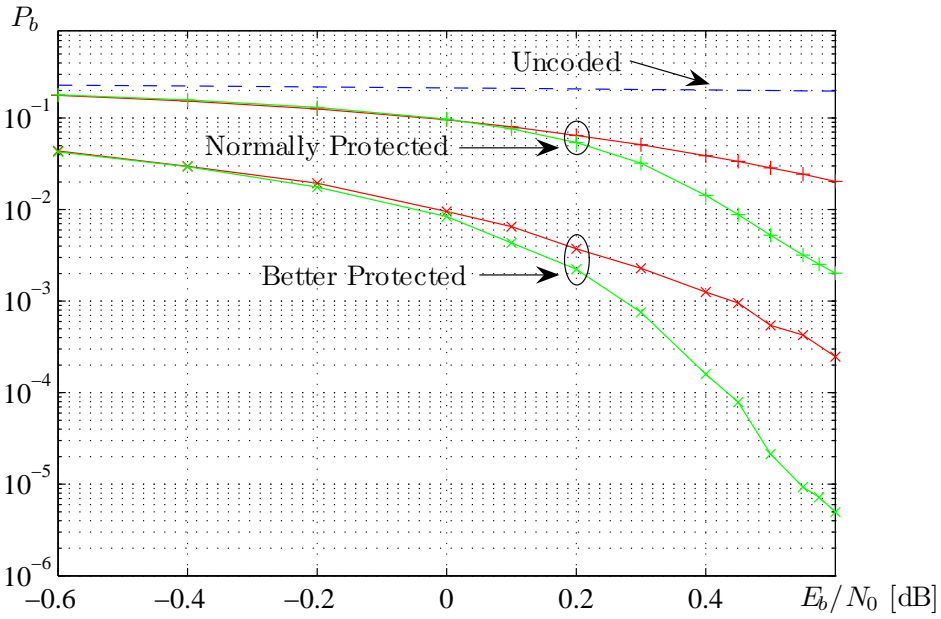


**Figure 12.** Bit error probabilities for the woven turbo scheme with permutation (green) and without permutation (red).

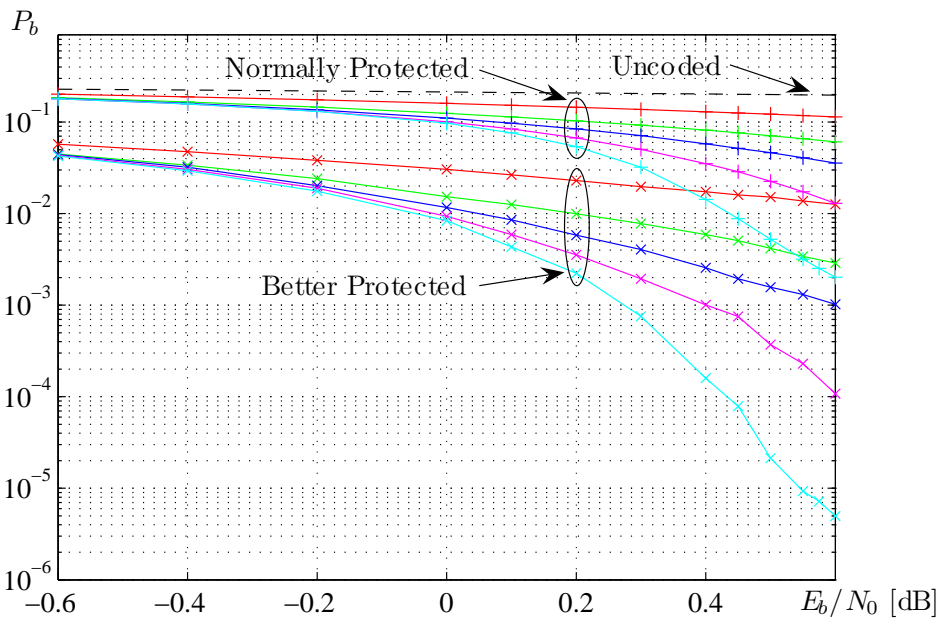


**Figure 13.** Bit error probabilities for both the normally protected and the better protected information symbols after 1 iteration (red), 2 iterations (green), 3 iterations (blue), 5 iterations (magenta), and 10 iterations (cyan), respectively.

As expected, the bit error probabilities are significantly worse in a good channel when the system does not use an intermediate permutation. However, unlike a classical turbo scheme the woven turbo scheme is still working (although with worse performance), showing its relation to the woven schemes.

#### 4.6. Different Number of Iterations

When dealing with iterative decoding procedures it is also important to know how fast a decoder converges to its decision. Previously, we always allowed to a woven decoder to perform 10 iterations assuming that this number is enough. Now we did the same calculations for 1, 2, 3, 5 iterations and compare the results with those after 10 iterations in the woven turbo decoder. Figure 13 demonstrates that even after 5 iterations the bit error performance can be improved significantly (approximately 0.2 dB) by allowing 5 more iterations. This shows that a really careful analysis of this issue has to be done while designing a communication system with woven turbo scheme.

### 5. CONCLUSIONS

In this paper we studied how to achieve unequal error protection for information symbols. To obey the requirements for an actual communication system two encoding schemes, *viz.*, a woven convolutional encoder and a woven turbo encoder, together with appropriate decoders were considered. In theory, either of the two schemes can be designed to possess unequal error protection when maximum-likelihood decoding is applied. It was shown that it is pretty easy to obtain two-level unequal error protection with any of them even if an iterative decoding procedure is used.

According to the results of our simulations, for the given system requirements the woven turbo scheme of rate  $R \approx 0.24$  outperforms its woven convolutional competitor with similar parameters and provides a coding gain of 4.17 dB over an uncoded transmission at  $P_b = 10^{-5}$  and satisfies the system requirements at 0.65 dB. However, if lower bit error probabilities would be required, the result of this comparison might be the opposite since the bit error rate curve for the woven convolutional encoder is much steeper in the waterfall region.

By increasing the rate of the constituent encoders in the “vertical” warp of the woven turbo encoder we also increase the overall rate. The woven turbo scheme of rate  $R \approx 0.32$  in the simulations appeared to perform a bit better than the previously considered woven turbo encoder of rate  $R \approx 0.24$  and it satisfies the system requirements already at 0.55 dB. Although neither the encoder nor the decoder are optimal, its performance at  $P_b = 10^{-5}$  is only 1.1 dB from the Shannon limit, which for  $R = 0.32$  is  $E_b/N_0 = -0.544$  dB.

Simulating the woven turbo scheme with identical constituent encoders in the “horizontal” warp, it was shown that the scheme’s error-correcting performance for the normally protected information symbols is not degraded due to the better protected symbols. It was also shown that the system performance is hardly affected by the number of constituent encoders in the warps and remains (nearly) the same with  $L = 10, 20, 30$ .

Since the goal of this paper was not to design a communication system for an existing technical project but to prove the effectiveness of our approach, for an actual communication system, a more careful analysis of the system parameters is still required. A larger number of different information protection levels can be similarly achieved by introducing larger variety of the constituent encoders in the horizontal warp.

### REFERENCES

1. Pavlushkov V., Johannesson R., Zyablov V.V. Unequal Error Protection for Convolutional Codes. *IEEE Trans. Inform. Theory*, submitted December 2004.
2. Johannesson R., Pavlushkov V., Zyablov V.V., Achieving Unequal Error Protection via Woven Codes: Construction and Analysis. *Information Processes* (<http://www.jip.ru/indexEng.htm>), to appear in May 2005.
3. Höst S., Johannesson R., Zyablov V.V., Woven Convolutional Codes I: Encoder Properties. *IEEE Trans. Inform. Theory*, 2002, vol. IT-48, no. 1, pp. 149–161.

4. Jordan R., Höst S., Johannesson R., Bossert M., Zyablov V.V. Woven Convolutional Codes II: Decoding Aspects. *IEEE Trans. Inform. Theory*, 2004, vol. IT-50, no. 10, pp. 2522–2529.
5. Freudenberger J., Bossert M., Zyablov V., Shavgulidze S. Woven Turbo Codes. *Algeb. and Combin. Coding Theory*. Banskó, Bulgaria, 2000, pp. 145–150.
6. Berrou C., Glavieux A., Thitimajshima P. Near Shannon Limit Error-Correcting Coding and Decoding: Turbo-Codes. *IEEE Int. Conf. Communications*. Geneva, Switzerland, 1993, pp. 1064–1070.
7. Shannon C.E. A Mathematical Theory of Communication. *Bell System Technical Journal*, 1948, vol. 27, pp. 379–423 (Part I), pp. 623–656 (Part II).
8. Lin S, Costello D.J.Jr. *Error Control Coding: Fundamentals and Applications*. Upper Saddle River, NJ: Pearson Prentice Hall, 2004, ed. 2nd.

*This paper was recommended for publication by V.I.Venets, a member of the Editorial Board*